Tuning the detection sensitivity: a model for axial backfocal plane interferometric tracking

Lars Friedrich and Alexander Rohrbach*

Laboratory for Bio- and Nano-Photonics, Institute for Microsystem Technology (IMTEK), University of Freiburg, Freiburg, Germany
**Corresponding author: rohrbach@imtek.uni-freiburg.de*

Received January 3, 2012; revised April 15, 2012; accepted April 15, 2012; posted April 16, 2012 (Doc. ID 160527); published June 1, 2012

Backfocal plane (BFP) interferometry is a single particle tracking technique that allows one to measure minute displacements of a microscopic particle from the center of a beam's focus in three dimensions. In this Letter, we present a Fourier optics model to describe the interference effects that allow one to track the position of a particle moving along the optical axis. A detection numerical aperture is derived theoretically and confirmed experimentally, within which the interference intensity has a positive correlation with the axial position of the scatterer. For larger detection angles, the correlation is negative. The model helps to understand previously reported measurements and to optimize BFP interferometric tracking. © 2012 Optical Society of America

OCIS codes: 120.0120, 140.7010, 260.3160, 290.0290.

Backfocal plane (BFP) interferometry [1,2] is a widely employed single particle tracking technique. It is typically combined with optical tweezers to precisely track three-dimensional displacements of the trapped particle from its equilibrium position. Many studies on single molecules utilize this technique, for example, to follow the transcription of DNA to RNA [3] as well as to show the stepping of molecular motors [4] or their mechanical properties [5].

The method relies on the coherent scattering of focused light at the particle to be tracked. The scattered light interferes with the unscattered excitation light and forms an intensity pattern that can be recorded to track the position of the scatterer. The interference pattern is observed in the BFP of a detection lens (DL), which forms a telescope with the focusing objective lens (OL).

A model for the formation of the tracking signals that encode the lateral displacement of a point scatterer perpendicular to the optical axis is given by Gittes and Schmidt [6]. Pralle *et al.* [1] present a model that also covers the formation of the axial tracking signal, which encodes the position of the scatterer along the optical axis. However, the model does not explain the dependency of the tracking sensitivity on the detection angle θ observed in simulation and measurement [7–9].

Here, we use Fourier optics to develop a new model for the BFP interference pattern for the case of a point scatterer located on the optical axis, which helps to maximize the sensitivity of axial tracking. The model predicts a detection angle $\theta_\varnothing$ at which the BFP intensity is independent of the particle position and thus explains the referenced observations.

The arrangement is sketched in Fig. 1. The focal electric field distribution $E_{i2}(r)$ can be computed from the angular spectrum $\tilde{E}_{i1}(k_\perp) = \mathrm{FT}\{E_{i1}(\varrho)\}$ of the incident plane wave $E_{i1}(\varrho) = \imath E_0$, which illuminates the BFP of the OL with a constant amplitude E_0. ϱ and r designate the distance to the optical axis in the BFP and the FP, respectively. For scalar fields one can assume radial symmetry.

$$\tilde{E}_{i1}(k_\perp) = 2\pi \int_0^{f\cdot \mathrm{NA_{OL}}} E_{i1}(\varrho) J_0(\varrho k_\perp)\varrho \mathrm{d}\varrho. \tag{1}$$

The focusing angle and thus the integration are limited by the numerical aperture $\mathrm{NA_{OL}}$ of the OL. Without loss of generality it is assumed that the OL and the DL have the same focal length f.

The Airy disk $E_{i2}(r)$ is obtained by rescaling $\tilde{E}_{i1}(k_\perp)$ according to [10].

$$E_{i2}(r) = \frac{1}{\imath\lambda_0 f}\tilde{E}_{i1}(k_\perp = rk_0/f), \tag{2}$$

$$= E_0 f \mathrm{NA_{OL}} \frac{J_1(\mathrm{NA_{OL}} k_0 r)}{r}, \tag{3}$$

where $k_0 = 2\pi/\lambda_0$ is the wavenumber of the incident light with vacuum wavelength λ_0.

A second application of the described formalism yields the field $E_{i3}(\varrho) = -\imath E_0$ in the BFP of the DL. Note that

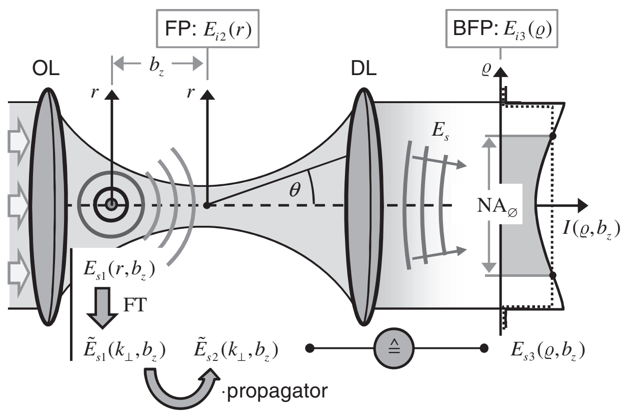

Fig. 1. An OL generates a field distribution $E_{i2}(r)$ in its focal plane (FP). A DL forms a telescope with the OL and converts the focused light to a field distribution $E_{i3}(\varrho)$ in its BFP. A scatterer located on axis at a position b_z from the FP gives rise to a field $E_{s1}(r, b_z)$ in the plane of the scatterer. The angular spectrum $\tilde{E}_{s1}(k_\perp, b_z)$ of the scattered field can be converted to the angular spectrum $\tilde{E}_{s2}(k_\perp, b_z)$ in the FP by multiplication with the propagator. Appropriate rescaling of $\tilde{E}_{s2}(k_\perp, b_z)$ yields the field distribution $E_{s3}(\varrho, b_z)$ in the BFP of the DL. θ denotes the detection angle. Indices i and s stand for incident and scattered.

the phase of $E_{i2}(r)$ is zero and the phase of $E_{i3}(\varrho)$ is $-\pi/2$ in agreement with the phase anomaly of focused light affecting $E_{i1}(\varrho)$ and $E_{i3}(\varrho)$.

We use a Gaussian beam approximation [11] for $E_{i2}(r)$ to estimate the phase of the focal field distribution along the optical axis. The Gaussian beam $E_{i2g}(r,z)$ reads

$$E_{i2g}(r,z=0) = E_{i2}(r=0)e^{-\left(\frac{r}{w_0}\right)^2} \approx E_{i2}(r). \tag{4}$$

By equating the second derivatives $\partial^2 E_{i2}(r)/\partial r^2$ and $\partial^2 E_{i2g}(r,z=0)/\partial r^2$ at $r=0$, the approximation is matched to the exact solution and the beam waist w_0 evaluates to the following:

$$w_0 = \frac{\sqrt{2}\lambda_0}{\pi \mathrm{NA}_{\mathrm{OL}}}. \tag{5}$$

The phase $\phi_g(z) = \arg\{E_{i2g}(r=0,z)\}$ of the focal field distribution along the optical axis is

$$\phi_g(z) = k_n z - \arctan\left(\frac{2z}{k_n w_0^2}\right). \tag{6}$$

$k_n = n_m k_0$ denotes the wavenumber inside the medium in the FP with refractive index n_m.

In the focal region the phase can be linearly approximated by $\phi_g(z) \approx z \cdot \bar{k}_z$. Even though the Gaussian beam model relies on a paraxial approximation and is not valid for large $\mathrm{NA}_{\mathrm{OL}}$, simulations show that the value

$$\bar{k}_z = \frac{\partial}{\partial z}\phi_g(z)\bigg|_{z=0} = k_n\left(1 - \left(\frac{\mathrm{NA}_{\mathrm{OL}}}{2n_m}\right)^2\right) \tag{7}$$

of the reduced axial wavenumber in the focus differs from the exact value by less than 10% for $\mathrm{NA}_{\mathrm{OL}} \le n_m 0.96$.

The particle to be tracked is located on the optical axis at a coordinate b_z with respect to the focal plane. It is modeled as a point scatterer that emits a spherical wave. For small displacements $|b_z| \ll \lambda_0/n_m$, the exciting amplitude can be approximated as constant while the initial phase of the scattered wave is $\bar{k}_z b_z$.

$$E_{s1}(r,b_z) = \frac{e^{\imath k_n r}}{-\imath k_n r} S_\perp \cdot e^{\imath \bar{k}_z b_z} \cdot E_{i2}(r=0). \tag{8}$$

The scattering parameter $S_\perp = -\imath k_n^3 \alpha/4\pi$ depends on the Clausius–Mossotti polarizability $\alpha = 3V(n_s^2 - n_m^2)/(n_s^2 + 2n_m^2)$ of the scatterer with volume V and refractive index n_s.

The angular spectrum

$$\tilde{E}_{s1}(k_\perp, b_z) = \frac{\imath k_n^2 \alpha}{\sqrt{k_n^2 - k_\perp^2}} \cdot e^{\imath \bar{k}_z b_z} \cdot E_{i2}(r=0) \tag{9}$$

of the scattered field is given by the Weyl representation $\mathrm{FT}\{\exp(\imath k_n r)/r\} = \imath 2\pi/\sqrt{k_n^2 - k_\perp^2}$ of a spherical wave [12].

The lower part of Fig. 1 outlines the concept to calculate the distribution $E_{s3}(\varrho, b_z)$ of the scattered field in the BFP of the DL. The angular spectrum $\tilde{E}_{s2}(k_\perp, b_z)$ of the scattered field in the FP is found by propagation of $\tilde{E}_{s1}(k_\perp, b_z)$, defined in the plane of the scatterer, by a distance b_z [13].

$$\tilde{E}_{s2}(k_\perp, b_z) = \tilde{E}_{s1}(k_\perp, b_z) \cdot e^{-\imath b_z \sqrt{k_n^2 - k_\perp^2}}. \tag{10}$$

According to the Fourier transformation property of the DL, $E_{s3}(\varrho, b_z)$ equals $\tilde{E}_{s2}(k_\perp, b_z)$ apart from the necessary scaling, introduced in Eq. (2).

The phase of the scattered light depends on the axial position b_z of the scatterer, enabling axial interferometric tracking:

$$\arg\{\tilde{E}_{s2}(k_\perp, b_z)\} = \frac{\pi}{2} + b_z\left(\bar{k}_z - \sqrt{k_n^2 - k_\perp^2}\right). \tag{11}$$

On the optical axis ($k_\perp = 0$), the phase of the scattered light is very sensitive on b_z because of the difference of the wavenumbers $\bar{k}_z$ and k_n of the incident and the scattered field.

However, Eq. (11) shows that there exists a detection direction $k_\perp = k_\varnothing$ at which the phase is independent of b_z.

$$\frac{\partial}{\partial b_z}\arg\{\tilde{E}_{s2}(k_\perp, b_z)\} \overset{!}{=} 0 \Rightarrow k_\varnothing = \sqrt{k_n^2 - \bar{k}_z^2}. \tag{12}$$

This direction corresponds to a detection angle $\theta_\varnothing = \arcsin(k_\varnothing/k_n)$.

In the BFP of the DL, the fields $E_{i3}(\varrho)$ and $E_{s3}(\varrho, b_z)$ interfere and form an intensity pattern:

$$I(\varrho, b_z) \propto |E_{i3}(\varrho)|^2 + |E_{s3}(\varrho, b_z)|^2 + 2\,\mathrm{Re}\{E_{i3}(\varrho) \cdot E_{s3}^*(\varrho, b_z)\}. \tag{13}$$

The term $|E_{s3}(\varrho, b_z)|^2$ can be neglected, since it is small compared to the two other summands.

To assess the performance of a tracking system that exploits the variations in $I(\varrho, b_z)$ to track a particle moving along the optical axis, it is helpful to introduce the normalized sensitivity

$$g_z(\varrho) = \frac{\partial}{\partial b_z}\frac{I(\varrho, b_z)}{I_0}\bigg|_{b_z=0} \tag{14}$$

of the intensity on the particle position. $I_0 \propto |E_{i3}(\varrho)|^2$ is the intensity in the BFP of the DL for no scatterer in the beam path. For the detection angle $\theta_\varnothing$ corresponding to $r_\varnothing = f n_m \sin(\theta_\varnothing)$, the sensitivity is $g_z(r_\varnothing) = 0$ since the scattered light is independent of b_z.

The theoretical value of g_z on the optical axis ($\varrho = 0$) can be determined by inserting the field

$$E_{s3}(\varrho = 0, b_z) = \frac{1}{\imath \lambda_0 f}\tilde{E}_{s2}(k_\perp = 0, b_z), \tag{15}$$

$$= E_0 \alpha \frac{n_m \pi^2 \mathrm{NA}_{\mathrm{OL}}^2}{\lambda_0^3} e^{-\imath b_z (k_n - \bar{k}_z)} \tag{16}$$

into Eq. (13) and replacing $\bar{k}_z$ according to Eq. (7):

$$g_z(\varrho = 0) = \mathrm{NA}_{\mathrm{OL}}^4 \frac{\alpha\pi^3}{\lambda_0^4}. \quad (17)$$

The strong dependence of g_z on the focusing numerical aperture $\mathrm{NA}_{\mathrm{OL}}$ arises from the fact that both the amplitude of the focal field $E_{i2}(r=0)$ exciting the scatterer and the reduced focal wavenumber $\bar{k}_z$ depend on $\mathrm{NA}_{\mathrm{OL}}^2$.

Figure 2 shows the results from a measurement that serves to illustrate the described effects. A polystyrene particle ($n_s = 1.57$) is attached to a glass coverslip and moved through a focus of a $\lambda_0 = 1064$ nm laser generated with a focusing numerical aperture $\mathrm{NA}_{\mathrm{OL}} = 1.2$ in water immersion ($n_m = 1.33$). For every axial position b_z of the particle, the intensity in the BFP of a detection lens (NA = 0.9) is recorded with a camera. The pixels of each frame are then binned according to their distance ϱ to the optical axis and normalized to the intensity I_0, which is obtained without the particle in the beam path.

The displayed data show that the correlation between small displacements $|b_z| \leq 500$ nm and the BFP intensity is positive for low detection angles θ and negative for high detection angles. The line profiles of $I(\varrho, b_z)$ presented in Fig. 2(a) further illustrate this well-known interrelation [8,9].

From the line profile at $\varrho_0 = 0.5$ mm the experimental on-axis sensitivity $g_z(\varrho = 0)$ can be estimated. It is a factor of 0.34 below the theoretical value 73.5 mm^{-1} obtained from Eq. (17). This deviation can be attributed to two effects. Because of the scalar theory used to determine $E_{i2}(r)$, the focal field is overestimated by approximately 10% since a significant fraction of the incident focused light is polarized along the optical axis and does not contribute to the interference. Furthermore, a Gaussian intensity profile was used to illuminate the BFP of the OL in the experiment instead of a plane wave $E_{i1}(\varrho) = \imath E_0$, reducing the effective focusing $\mathrm{NA}_{\mathrm{OL}}$.

Figure 2(c) shows the experimental course of $g_z(\varrho)$. It has a zero crossing at $\theta = 34.2°$, which is close to $\theta_\varnothing = 37°$ predicted by the theory introduced here.

In a typical tracking system, a circular detector located in the BFP of the DL integrates the central part of $I(\varrho, b_z)$ and thereby generates a tracking signal encoding the axial position b_z of the tracked particle. For practical applications, a high value of $g_z(\varrho)$ is desirable to achieve a strong signal compared to noise arising from fluctuations of the incident light power.

The results of this study show that the numerical aperture of the tracking system should be smaller than $\mathrm{NA}_\varnothing = n_m \sin(\theta_\varnothing)$, so that only the region with positive sensitivity $g_z(\varrho) > 0$ is recorded (see right side of Fig. 1). Inserting Eq. (7) into Eq. (12) allows one to derive the convenient first order approximation

$$\mathrm{NA}_\varnothing \approx \frac{\mathrm{NA}_{\mathrm{OL}}}{\sqrt{2}} \quad (18)$$

for the crucial detection numerical aperture.

In conclusion, we presented a theoretical approach that explains the previously observed [7,8] dependency of the axial tracking sensitivity on the detection angle. The sensitivity of tracking systems can be optimized by selecting detection angles smaller than the derived angle $\theta_\varnothing$, at which the sensitivity is zero. If exclusively detection angles $\theta > \theta_\varnothing$ are used, a negative sensitivity is obtained that allows axial tracking as well. Recording the intensity pattern at detection angles $\theta \approx \theta_\varnothing$ yields a measure for the incident laser power, irrespective of the position of the tracked particle. This measure can be used as a reference, similar to the approach in [14]. The listed applications of the presented results enable more precise three-dimensional tracking of small particles.

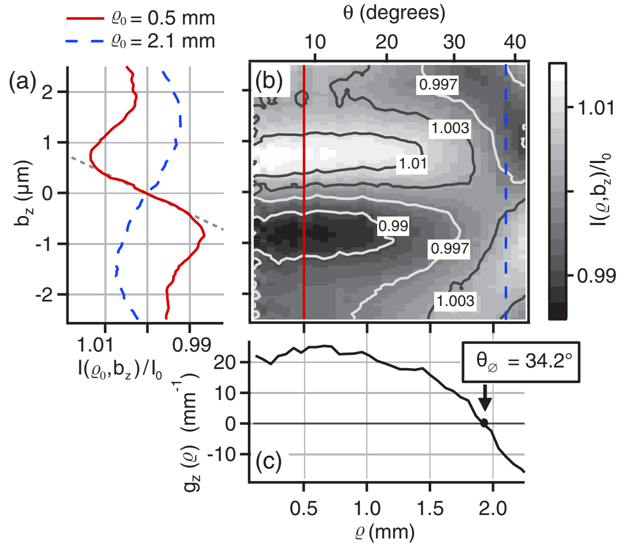

Fig. 2. (Color online) A polystyrene particle with radius 100 nm is moved through a focus. (b) The intensity distribution $I(\varrho, b_z)$ in the BFP of a DL is displayed as a function of the distance ϱ to the optical axis and the axial position b_z of the scattering particle with respect to the focal position. (a) Line profiles at two distinct detection angles. A linear fit (dashed line) indicates $g_z(\varrho = 0.5\ \mathrm{mm}) = 25.3\ \mathrm{mm}^{-1}$. (c) Sensitivity $g_z(\varrho)$ is determined from (b).

References

1. A. Pralle, M. Prummer, E. Florin, E. Stelzer, and J. Hoerber, Microsc. Res. Tech. **44**, 378 (1999).
2. A. Rohrbach and E. Stelzer, J. Appl. Phys. **91**, 5474 (2002).
3. K. Neuman, E. Abbondazieri, R. Landick, J. Gelles, and S. Block, Cell **115**, 437 (2003).
4. V. Bormuth, V. Varga, J. Howard, and E. Schaffer, Science **325**, 870 (2009).
5. N. Becker, S. Altmann, T. Scholz, J. Hoerber, E. Stelzer, and A. Rohrbach, Phys. Rev. E **71**, 021907 (2005).
6. F. Gittes and C. Schmidt, Opt. Lett. **23**, 7 (1998).
7. A. Rohrbach, H. Kress, and E. Stelzer, Opt. Lett. **28**, 411 (2003).
8. J. Dreyer, K. Berg-Sorensen, and L. Oddershede, Appl. Opt. **43**, 1991 (2004).
9. A. Samadi and S. Reihani, Opt. Lett. **36**, 4056 (2011).
10. J. Goodman, *Introduction to Fourier Optics* (Roberts and Company, 2005), Chap. 5, p. 103.
11. B. Saleh and M. Teich, *Fundamentals of Photonics* (Wiley Interscience, 2007), Chap. 3, p. 74.
12. L. Mandel and E. Wolf, *Optical Coherence and Quantum Optics* (Cambridge Univ., 1995), Chap. 3, p. 120.
13. J. Harvey, Am. J. Phys. **47**, 974 (1979).
14. L. Friedrich and A. Rohrbach, Opt. Lett. **35**, 1920 (2010).